MS PAGE 637-638 MISSING

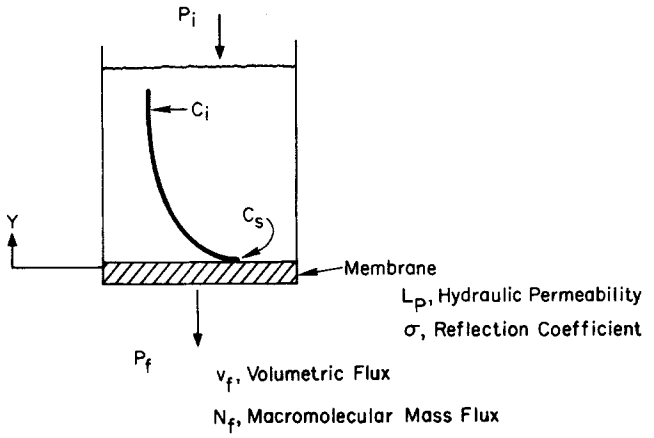

Figure 1. Schematic diagram showing solute concentration profile in the polarization layer formed during ultrafiltration is an unstirred cell.

drodynamics from the theoretical analysis.

Analysis of ultrafiltration in an unstirred cell requires a solution of the one-dimensional time-dependent convective diffusion equation as applied to the polarization layer on the solute-rich side of the membrane. Williams (1969) used regular perturbation theory to find asymptotic solutions for this in the context of reverse osmosis. The asymptotic solution predicts that, for times much larger than $t = D/(L_p\Delta P)^2$, solvent flux will decay like $t^{-1/2}$. For shorter times, both Williams and Mahlab et al. (1978, 1979) have developed alternate solutions which are valid if $(\Delta P - \Delta\pi_i)/\Delta P$ is much less than unity. The experiments of Liu and Williams (1970) and of Mahlab et al. (1979) give some indication of the range of parameters, including membrane solute rejection, for which these short time solutions apply but, like the investigations of Alfani and Drioli (1972), these experiments show the difficulty of testing the long time solution in reverse osmosis experiments. Recently, a long time solution has also been derived by Trettin and Doshi (1980) for the same problem of albumin ultrafiltration in an unstirred cell which we investigate here. Their solution, based on the assumption of gel layer formation upon the membrane, predicts ultrafiltrate flux decay like $t^{-1/2}$ and that albumin concentration at the membrane surface is independent of ΔP. Experimental data are offered in support of the flux decay rate only. In our work, the long time results of Williams are slightly generalized and a novel solution is developed for the case in which a macromolecular gel layer forms upon the membrane. Most important, data are offered in direct experimental support of the model.

ANALYSIS

Problem Statement

Figure 1 is a conceptual diagram of ultrafiltration in an unstirred cell. The fluid above the membrane is initially static and contains a uniform concentration of macromolecule. The membrane is slightly permeable to the macromolecule, and is characterized by σ, the reflection coefficient, L_p, the hydraulic permeability, as well as the diffusive permeability. At time zero, the solution is subjected to a constant elevated pressure such that the pressure differential across the cell, $\Delta P = P_i - P_f$ gives rise to an ultrafiltrate volumetric flux and a macromolecular mass flux, v_f and N_f, respectively. Solute rejection at the membrane leads to a macromolecular concentration profile, $c(y, t)$, in the polarized layer above the membrane.

The objective of this analysis, which is presented in three parts, is to obtain expressions for $c(y, t)$ and $v_f(t)$ for thermodynamically limited and hydrodynamically limited ultrafiltration. These solutions can then be compared with the experimental measurements. The first of the three problems is to solve for the macromolecule concentration profile and ultrafiltrate flux if the membrane is highly rejecting and the gelling concentration is not exceeded. In the second problem, a solution is developed for the steady state which is attained if the rate of solute leakage through the membrane can equal the rate of convection of solute toward the membrane. In the third problem we solve for the profile and flux in the polarization layer above an impermeable membrane upon which there forms an insoluble, ever-thickening, gel-like layer of constant concentration c_g. Constant density ρ and solute diffusivity D are assumed. The unsteady state one-dimensional convective diffusion equation is:

$$\frac{\partial c}{\partial t} - v\frac{\partial c}{\partial y} = \frac{\partial^2 c}{\partial y^2} \tag{1}$$

subject to:

$$c = c_i \quad \text{all } y,\ t = 0 \tag{2}$$

$$c = c_i \quad y \to \infty,\ \text{all } t \tag{3}$$

The remaining boundary condition for c at $y = 0$ and the expression for v distinguish the permeable membrane and gel formation problems.

Highly Rejecting Membrane. The solute flux N_f through the membrane is given by:

$$N_f = (1 - R)v_f c_s \tag{4}$$

where the rejection coefficient

$$R \equiv 1 - \frac{c_f}{c_s} \tag{5}$$

depends on the magnitude of the reflection coefficient and the membrane Peclet number (Spiegler and Kedem, 1966; Anderson and Quinn, 1974). In this problem, we assume that R is constant and almost equal to one, as was the case in our experiment. The net flux to the membrane from the bulk solution must be equal to the flux through the membrane, as given by Eq. 4, i.e.,

$$D\frac{\partial c}{\partial y} + vc = (1 - R)v_f c \quad y = 0,\ \text{all } t \tag{6}$$

The convective velocity v above the membrane and ultrafiltrate volumetric flux v_f differ because the densities of the fluids on either side of the membrane differ. The ultrafiltrate volumetric flux is assumed proportional to the difference between the applied pressure and the effective osmotic pressure difference between the two solutions on each side of the membrane, so that:

$$v_f = L_p[\Delta P - \sigma\Delta\pi] \tag{7a}$$

where $\Delta\pi = \pi_s - \pi_f$. The velocity v in the polarization layer is related to the ultrafiltrate velocity by:

$$v\rho = v_f\rho_f \tag{7b}$$

where ρ is assumed constant and is evaluated as the average of the densities of the bulk solution and of the solution at the membrane surface. For the experimental conditions investigated, $\rho/\rho_f \leq 1.09$ (Vilker, 1975).

An asymptotic solution to Eqs. 1, 2, 3, 6, 7a and 7b is sought for some long time at which the membrane surface concentration c_s approaches the concentration c^* for which $[\Delta P - \sigma\Delta\pi] = 0$. Order-of-magnitude analysis of these equations suggests that the polarized boundary layer thickness is proportional to $(Dt)^{1/2}$ and the convective velocity is proportional to $(D/t)^{1/2}$. A convenient set of dimensionless dependent variables is therefore,

$$\theta = \frac{c - c_i}{c^* - c_i} \tag{8}$$

$$V = v(t/D)^{1/2} \tag{9}$$

$$\xi = y/(Dt)^{1/2} \tag{10}$$

$$\eta = L_p[\Delta P - \sigma\Delta\pi_i](t/D)^{1/2} \tag{11}$$

which lead to

$$\frac{\eta}{2}\frac{\partial\theta}{\partial\eta} - \left(\frac{\xi}{2} + V\right)\frac{\partial\theta}{\partial\xi} = \frac{\partial^2\theta}{\partial\xi^2} \tag{12}$$

with boundary conditions

$$\theta = 0 \quad \text{all } \xi,\ \eta = 0 \tag{13}$$

$$\theta \to 0 \quad \xi \to \infty, \text{ all } \eta \tag{14}$$

$$\frac{\partial\theta}{\partial\xi} + V\left[\theta + \frac{c_i}{c^* - c_i}\right]$$

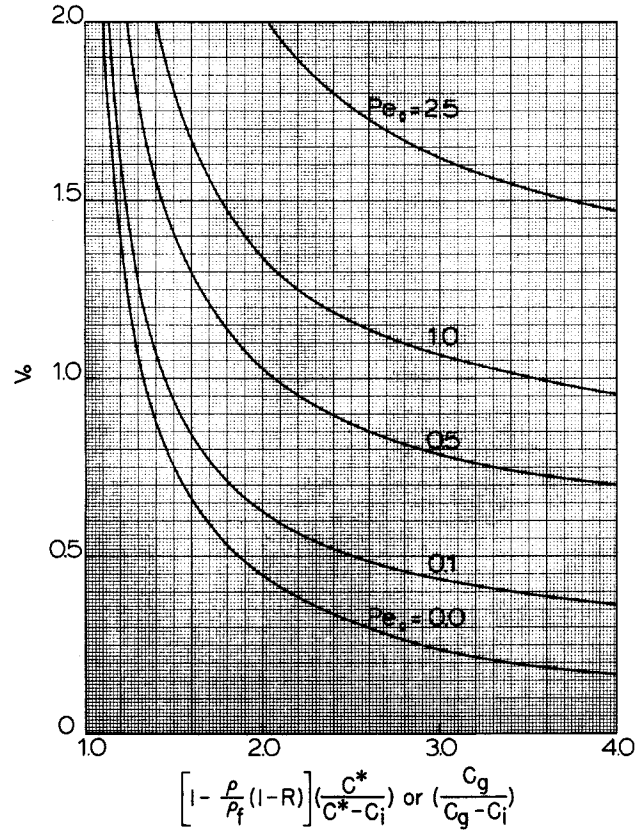

Figure 2. Solution of Eq. 22 or 46 for the ultrafiltrate flux parameter V_o.

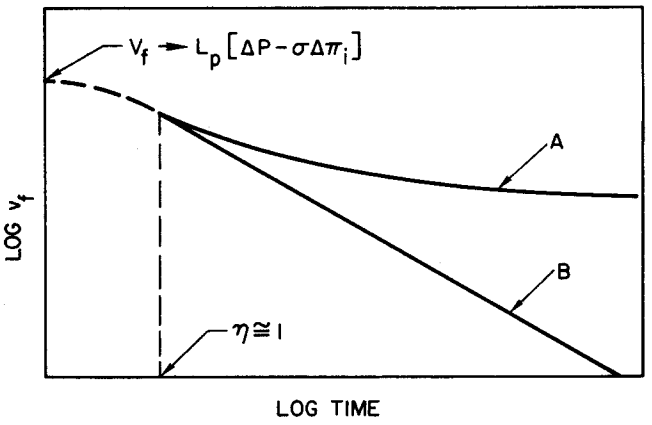

Figure 3. Qualitative description of ultrafiltrate flux decay in unstirred ultrafiltration for a relatively leaky membrane (Curve A) such that $(v_f/v)c^* > c_i/(1-R)$ for which the flux becomes constant, and for a highly rejecting membrane (Curve B) such that $(v_f/v)c^* < c_i/(1-R)$ for which the flux decays like $t^{-1/2}$ at long times. At short times ($\eta << 1$), both curves approach the limiting flux, $v_f \to L_p[\Delta P - \sigma\Delta\pi_i]$.

$$= (1 - R)\frac{\rho}{\rho_f}V\left[\theta + \frac{c^*}{c^* - c_i}\right] \quad \xi = 0, \text{ all } \eta \tag{15}$$

$$V = \frac{\rho_f[\Delta P - \sigma\Delta\pi]}{\rho[\Delta P - \sigma\Delta\pi_i]}\,\eta \tag{16}$$

For the purpose of examining behavior at long times, it is important to note that the expected solution will require that $\Delta P - \sigma\Delta\pi \to 0$ as $t \to \infty$. Therefore, if c^* is that concentration for which $\Delta P - \sigma\Delta\pi = 0$, it will suffice to approximate $\Delta\pi$ by:

$$\Delta\pi = \frac{\Delta P}{\sigma} - \left(\frac{\partial\Delta\pi}{\partial c}\right)^*(c^* - c_s) \tag{17}$$

and Eq. 16 becomes

$$V = \frac{\rho_f}{\rho}\left[\sigma\left(\frac{\partial\Delta\pi}{\partial c}\right)^*\right]\frac{c^* - c_i}{\Delta P - \sigma\Delta\pi_i}(1 - \theta)\eta \tag{18}$$

Consequently, the long time behavior of the solution does not require linearity of π vs. c over the entire range of realizable concentrations. Instead, the linearization is required only in the vicinity of c^*. Solutions valid for $\eta >> 1$ are sought of the form

$$\theta(\xi) = \sum_{j=0} \eta^{-j}\theta_j(\xi) \tag{19}$$

$$V = \sum_{j=0} \eta^{-j}V_j \tag{20}$$

The problem reduces to finding the functions $\theta_j(\xi)$ and terms V_j. The technique involves substitution of the first few terms of Eqs. 19 and 20 in 12, 15, and 18 and requiring that coefficients of powers of η independently go to zero. Details are available in Vilker (1975). The results are

$$\theta = \frac{1 - erf\{\xi/2 + V_o\}}{1 - erf\, V_o} \tag{21}$$

and V_o is given implicitly by:

$$\frac{\exp(-V_o^2)}{V_o(1 - erf\, V_o)} = \sqrt{\pi}\left[1 - \frac{\rho}{\rho_f}(1 - R)\right]\frac{c^*}{c^* - c_i} \tag{22}$$

For $R = 1$, Eq. 22 is plotted in Figure 2 as the curve corresponding to $Pe_g = 0$.

As anticipated, these results predict that ultrafiltrate flux decays like $t^{-1/2}$ and that the membrane surface concentration is approximately equal to the concentration for which the solution osmotic pressure equals the applied pressure. We also see that the thickness of the polarized layer grows like $t^{1/2}$.

Relatively Leaky Membrane. If the membrane is relatively leaky, it is possible that solute transport through the membrane can equal convection of solute to the membrane: i.e., if,

$$\frac{v_f}{v}c^* > \frac{c_i}{1 - R} \quad \text{or} \quad \frac{\rho}{\rho_f}c^* > \frac{c_i}{1 - R}$$

then c_s will not attain the value c^*. A steady state will instead be established with

$$c_s = \frac{1}{1 - R}\frac{\rho_f}{\rho}c_i \tag{23}$$

Ultrafiltrate flux can then be evaluated from Eq. 7a and appropriate osmotic pressure data. In this event, the concentration profile is given by:

$$\theta = \exp\{-vy/D\} \tag{24}$$

where it is to be understood that θ is referenced to c_s rather than c^*. Figure 3 compares the qualitative behavior of the ultrafiltrate flux expected for the two cases of interest

$$\frac{v_f}{v}c^* < \frac{c_i}{1 - R} \quad \text{and} \quad \frac{v_f}{v}c^* > \frac{c_i}{1 - R}$$

Gel Formation Model. At sufficiently high applied pressure, it has been suggested that the concentrated macromolecular solution at the membrane surface undergoes a phase transition. The resulting gel layer, which thickens with time and with further increase in applied pressure, offers an additional resistance to hydraulic flow. We assume that the concentration of macromolecule in this layer, c_g, and the gel permeability, B_g, are constant. The membrane is assumed impermeable to the macromolecule ($R = \sigma = 1$). The volumetric flux through the gel layer is:

$$v = \frac{B_g}{l_g}\,\Delta P_g \tag{25}$$

where l_g is gel layer thickness and ΔP_g is the gel layer pressure drop which contributes to the overall pressure drop

$$\Delta P = \Delta P_m + \Delta P_g \tag{26}$$

For constant solution density and diffusivity in the polarization layer above the gel, Eqs. 1-3 again apply, but the analogs to Eqs. 4 and 7 are:

$$D\frac{\partial c}{\partial y} + vc = c_g\frac{dl_g}{dt} \quad y = l_g, \text{ all } t \tag{27}$$

$$v = \frac{\rho_f}{\rho}\,L_p(\Delta P_m - \Delta\pi) \tag{28}$$

where $\Delta\pi = \pi_s - \pi_f$. After gel formation, π_s is evaluated at c_g, $\Delta\pi = \pi_g - \pi_f$.

Substitution of the dimensionless groups

$$\theta = (c - c_i)/(c_g - c_i) \tag{29}$$

$$\xi = (y - l_g)/(Dt)^{1/2} \tag{30}$$

$$\eta = L_p(\Delta P - \Delta\pi)(t/D)^{1/2} \tag{31}$$

$$V = v(t/D)^{1/2} \tag{32}$$

$$\mathcal{L} = l_g/(Dt)^{1/2} \tag{33}$$

into Eq. 1 and the other constraints gives

$$\frac{\eta}{2}\frac{\partial\theta}{\partial\eta} - \left\{\frac{\xi}{2} + \frac{\mathcal{L}}{2} + V + \frac{\eta}{2}\frac{d\mathcal{L}}{d\eta}\right\}\frac{\partial\theta}{\partial\xi} = \frac{\partial^2\theta}{\partial\xi^2} \tag{34}$$

subject to:

$$\theta = 0 \quad \text{all } \xi,\ \eta = 0 \tag{35}$$

$$\theta \to 0 \quad \xi \to \infty, \text{ all } \eta \tag{36}$$

$$\frac{\partial\theta}{\partial\xi} + V\left[\theta + \frac{c_i}{c_g - c_i}\right] = \frac{c_g}{c_g - c_i}\left[\frac{\mathcal{L}}{2} + \frac{\eta}{2}\frac{d\mathcal{L}}{d\eta}\right] \quad \xi = 0, \text{ all } \eta \tag{37}$$

$$V = \frac{B_g(\Delta P - \Delta\pi)}{D\mathcal{L}}\left[1 - \frac{f(\eta)}{\eta}\right] \tag{38a}$$

$$V = \frac{\rho_f}{\rho}\left[\frac{\Delta P_m - \Delta\pi}{\Delta P - \Delta\pi}\right]\eta = \frac{\rho_f}{\rho}\,f(\eta) \tag{38b}$$

The last boundary condition has been simplified by:

$$\Delta P_m = \Delta\pi + (\Delta P - \Delta\pi)\frac{f(\eta)}{\eta} \tag{39}$$

With perturbation techniques, asymptotic solutions valid for $\eta >> 1$ are sought of the form:

$$\theta = \sum_{j=0} \eta^{-j}\theta_j(\xi) \tag{40}$$

$$\mathcal{L} = \sum_{j=0} \eta^{-j}\mathcal{L}_j \tag{41}$$

$$f = \sum_{j=0} \eta^{-j}f_j \tag{42}$$

$$V = \sum_{j=0} \eta^{-j}V_j \tag{43}$$

Following the method described above, the first terms of Eqs. 40-43 give the results:

$$\theta_o = \frac{1 - erf\left\{\frac{\xi}{2} + \frac{\mathcal{L}_o}{2} + V_o\right\}}{1 - erf\left\{\frac{\mathcal{L}_o}{2} + V_o\right\}} \tag{44}$$

$$V_o = \frac{B_g(\Delta P - \Delta\pi)}{\mathcal{L}_o D} \tag{45}$$

and V_o (which is equal to $\rho_f f_o/\rho$ by Eq. 38b) is given implicitly by:

$$\frac{\exp\left\{-\left[\frac{Pe_g}{2V_o} + V_o\right]^2\right\}}{V_o\left(1 - erf\left\{\frac{Pe_g}{2V_o} + V_o\right\}\right)} = \sqrt{\pi}\,\frac{c_g}{c_g - c_i}\left[1 - \frac{Pe_g}{2V_o^2}\right] \tag{46}$$

where

$$Pe_g = \frac{vl_g}{D} = \frac{B_g(\Delta P - \Delta\pi)}{D} \tag{47}$$

is a gel layer Peclet number. Obviously, for $Pe_g = 0$, Eq. 46 reduces to Eq. 22 with $R = 1$. The consequences of $Pe_g \neq 0$ are shown in Figure 2.

As in the absence of the gel layer, the ultrafiltrate flux retains its inverse square root dependence on time, and the concentration polarization layer still grows with a square root dependence on time. Like the polarization layer, the gel layer thickness also increases with the square root of time. Equation 45 and Figure 2 suggest that, after gel formation, flux can be increased for any constant value $c_g/(c_g - c_i)$ by increasing Pe_g. Increasing applied pressure, ΔP, would increase Pe_g, but the conclusion that this change would result in higher ultrafiltrate flux is inconsistent

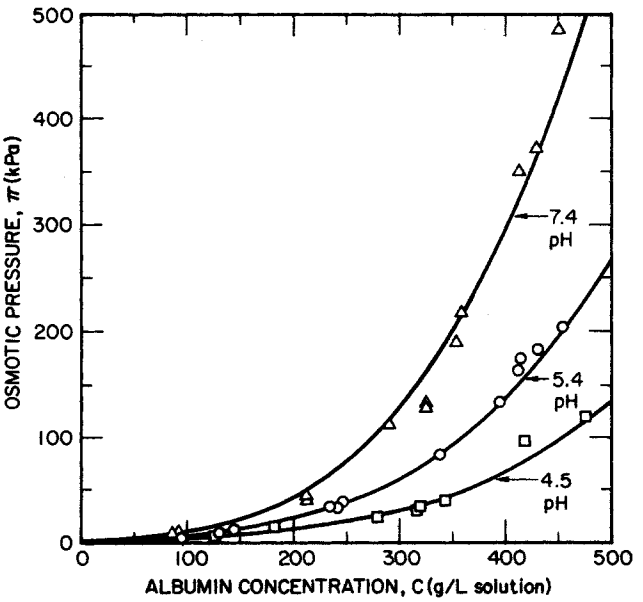

Figure 4. Albumin osmotic pressure as a function of albumin concentration at 25°C and in 0.15 M NaCl at pH 7.4 (Δ), pH 5.4 (○) and pH 4.5 (□). Semiempirical curves through data at each pH are derived in Vilker et al, (1981a).

TABLE 1. ULTRAFILTRATION EXPERIMENT SUMMARY

	Experiments at pH 4.5				Experiments at pH 5.4				Experiments at pH 7.4		
	A	B	C	D	E	F	G	H	I	J	K
CONTROLLED PARAMETERS											
Bulk Solution Concentration, c_i, g/L solution	101	101	110	110	158	64	101	101	72	101	101
Total Experiment Time, minutes	547	563	1368	1387	134	677	548	540	535	548	529
Profile Measurement Time, minutes	540	542 555	542 1368	1387	33 88	648	no data	532	531	544	529
Membrane Permeability, $L_p \times 10^4$, cm/kPa-min	6.1	9.1	6.8	3.0	12.3	4.8	5.1	9.1	5.4	9.3	7.8
Cell Pressure Difference, ΔP, kPa	70	70	70	276	39	70	70	70	69	70	70
Osmotic Equivalent Concentration, c^*, g/L solution	405	405	405	652	251	312	312	312	241	242	242
Average Polarization Layer Density, ρ, g/mL	1.06	1.06	1.06	1.09	1.05	1.05	1.05	1.05	1.04	1.04	1.04
Diffusivity at Average ϕ, Eq. 49, $D \times 10^7$, cm²/s	1.7	1.8	1.7	1.2	2.1	2.4	2.1	2.1	2.6	2.5	2.5
CONCENTRATION PROFILE DATA											
Membrane Surface Concentration, c_s, g/L solution	416	389 399	387 380	581	260 260	345	no data	320	261	248	250
Polarization Layer Thickness, δ, cm	0.280	0.260 0.260	0.375 0.430	0.375	0.140 0.210	0.350	—	0.340	0.325	0.400	0.400
Apparent Diffusivity Fit to Profile, $D \times 10^7$, cm²/s	16	10	10	10	30	30	—	20	30	30	30
FLUX DATA											
Fitted Power of Time, $-n$	0.536	0.558	0.494	0.509	no data	0.491	0.476	0.469	0.427	0.464	0.429
Fitted Coefficient $A_o \times 10^3$, cm/(min)$^{n+1}$	4.9	5.0	4.2	5.7	—	6.1	4.9	5.4	7.3	5.7	5.7
Coefficient for $n = -1/2$, $A_o \times 10^3$, cm/min$^{1/2}$	4.22	3.90	4.36	5.42	—	6.35	5.44	6.20	10.17	6.68	7.60
Apparent Diffusivity for $n = -1/2$, $D \times 10^7$, cm²/s	2.7	2.3	2.3	2.2	—	4.3	7.4	9.6	22.9	20.4	26.5

with the experimental findings of others (e.g., Blatt et al., 1970). Generally it has been supposed that, after gel formation occurs, further increases in applied pressure result in a thickening of the gel layer such that the increased hydraulic resistance of the gel approximately offsets the increased driving force, and flux remains relatively unchanged. The assumption of a pressure independent intrinsic gel permeability in our model is probably the reason for the over prediction of a substantial increase in flux in response to an increase in applied pressure.

It is also somewhat counter-intuitive to note that the role of the gel may be to increase ultrafiltrate flux. That is, for two solutes which are identical in all respects except that $c_g < c^*$ for one and $c_g > c^*$ for the other, it is possible that the gel-forming solute will actually permit the greater flux of solvent.

EXPERIMENTAL

Experiments were performed to measure ultrafiltrate flux and concentration profiles in the polarization layer. The system of bovine serum albumin (BSA) dissolved in 0.15 M NaCl was selected because of the extensive physicochemical data available. However, measurements of solution density and osmotic pressure had to be extended to higher albumin concentrations than could be found in the literature (Vilker, 1975; Vilker et al., 1981a). The hydrated BSA partial specific density remained constant at 1.340 ± 0.005 g/cc up to c = 580 g/L and the solution density followed the relation

$$\rho = 2.54 \times 10^{-4} c + 1.00 \qquad (48)$$

Osmotic pressure data as a function of concentration and solution pH, extended to high albumin concentrations (Vilker et al., 1981a), are shown in Figure 4.

Albumin diffusivity data in salt solutions are available from Keller et al. (1971). Their results for BSA dissolved in acetate buffer near the isoelectric pH of approximately 4.7 are described by the empirical relation

$$D/D_\infty = (\tanh 21.3\phi)/21.3\phi \qquad (49)$$

where the infinite dilution diffusivity, D_∞, is 7×10^{-7} cm²/s, and the volume fraction of albumin is given by $\phi = c/1340$.

Materials

Albumin solutions were prepared by dissolving crystallized BSA (Pentex grade, Miles Laboratories) in 0.15 M NaCl solutions which had been previously ultrafiltered (PM-10 membrane, nominal molecular weight cut-off 10,000, Amicon Corporation, Lexington, MA). Solution pH adjustments were made with purified hydrochloric acid or sodium hydroxide solutions. After pH adjustment, the solutions were passed through a 0.1 μm filter as a final precaution. Initial BSA concentration in the cell was determined by the Biuret method (Henry, 1964).

Cellulosic sheet membranes (HFA-180, Abcor Corporation, Wilmington, MA) were used for all experiments. This membrane was selected for its ruggedness and pliability, almost complete albumin rejection (>0.99), and negligible rejection of NaCl.

Apparatus and Procedures

The unstirred optical ultrafiltration cell and the method for obtaining concentration profile measurements has been described in the companion paper (Vilker, et al., 1981b). The cell was capable of withstanding pressure to 350 kPa. Total membrane area was 1.524 cm². Ultrafiltrate flux measurements were made with a continuous low flow measuring device which was capable of measuring flow rates from 10^{-5} to 10^{-1} mL/min (Vilker et al., 1979). The moment at which pressure was applied to the ultrafiltration cell was taken as time zero. Flux measurements

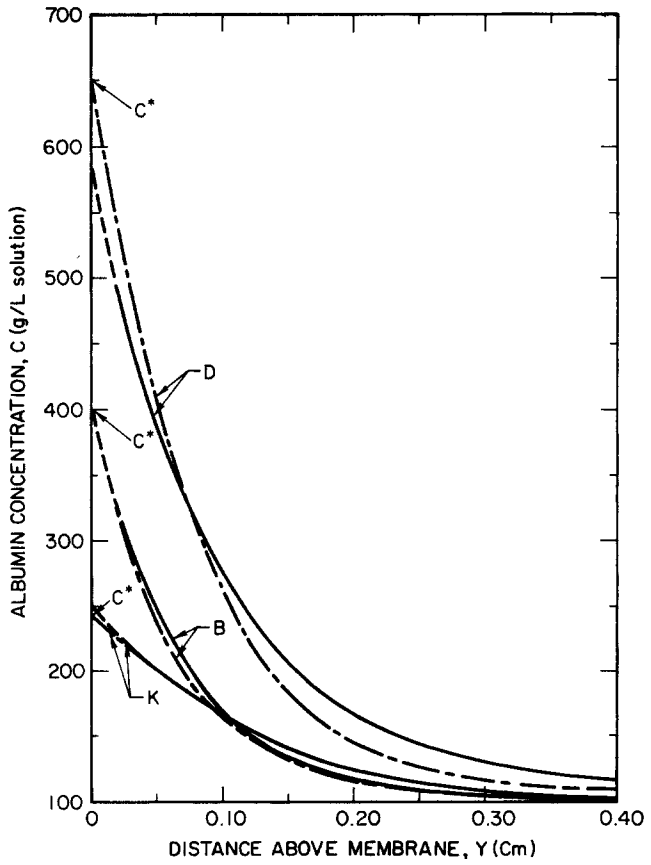

Figure 5. Experimental (———) and theoretical (— — —) albumin concentration profiles in polarized layer showing the effect of applied pressure. Experiment D, pH 4.5, ΔP = 276 kPa; Experiment B, pH 4.5, ΔP = 70 kPa; Experiment K, pH 7.4, ΔP = 70 kPa.

could be obtained within about 3 seconds after pressure application. Total ultrafiltrate volume from a typical experiment was 0.5 mL.

Prior to each experiment, all cell components were thoroughly rinsed with water which had been previously ultrafiltered using an Amicon PM10 membrane. The hydraulic permeability constant, L_p, was determined before and after each experiment with ultrafiltered saline. Experiments were performed at approximately 25°C. During each experiment, ambient temperature was controlled to ±0.1°C in order to minimize natural convection effects in the ultrafiltration cell and to ensure proper flow measurement readings.

RESULTS AND DISCUSSION

Eleven experiments were performed to investigate the effects of bulk solution pH and albumin concentration, applied pressure, and elapsed time on the ultrafiltration flux and BSA concentration profiles. Table 1 summarizes the experimental conditions investigated and some of the results obtained. Experiments A and B (pH 4.5), Experiment H (pH 5.4), and Experiments J and K (pH 7.4) permit evaluation of the effect of solution pH at equivalent conditions of bulk solution albumin concentration and applied pressure. Changes in BSA concentration profiles with increasing elapsed time are investigated in Experiments C and E. Experiment D at high pressure and pH 4.5 is designed to encourage the formation of a protein gel layer at the membrane surface.

The solid curves of Figure 5 for Experiments B, D and K show typical albumin concentration profiles measured by the shadowgraph method. Each solid curve is the average of two independent measurements which agreed within five percent or better of each other at all concentrations. Since concentration measurements were not possible for $y < 0.02$ cm, the membrane surface concentration, c_s, was obtained by extrapolation of the profile data as previously described (Vilker et al., 1981b). Regardless of the level of applied pressure or the value of bulk solution pH, these data show that the extrapolated membrane surface concentration agrees closely with the osmotic equivalent concentration; that is, within experimental error $c_s \simeq c^*$. This same conclusion applies to the other experiments in Table 1 for all conditions studied. These membrane surface concentration measurements suggest that an insoluble gel-type layer at the membrane surface was not present in any of our experiments.

Experiment D was conducted at conditions thought to be favorable for gel formation and growth above the 0.02 cm viewing limitation. Literature estimates of albumin solubility close to the isoelectric pH of 4.7 are 610 g/L from dissolution studies of albumin in water by MacRitchie (1973) and 585 g/L from viscosity studies by Kozinski and Lightfoot (1972). At this assumed gel concentration (c_g = 600 g/L), the osmotic pressure for pH 4.5 is estimated as 216 kPa by extrapolation of the data given in Figure 4. A run at pH 4.5 and ΔP = 276 kPa, which should have been more than sufficient to encourage incipient gel formation, was therefore undertaken. As shown by solid curve D of Figure 5, there was no evidence of gel formation even after 1300 minutes of elapsed time. The applied pressure was then increased to 350 kPa for an additional 900 minutes; again with no evidence of gel formation.

Given that gel formation was absent and that the membranes were highly rejecting to albumin ($R \sim 1.0$), Equation 21 should provide an appropriate description of the experimental concentration profiles, provided only that η is sufficiently large ($\eta >> 1$). For ultrafiltration of biological macromolecules such as albumin, the minimum time for $\eta \simeq 1$ is small. In our experiments, it is typically about one second for experiments at low pressures and about one-tenth second for the experiment at high pressure.

The dashed curves of Figure 5 show concentration profiles calculated by Eq. 21 with apparent values of diffusivity which provide a good fit between theoretical prediction and experimental data: for Experiments B and D, $D = 10 \times 10^{-7}$ cm²/s; for Experiment K, $D = 30 \times 10^{-7}$ cm²/s. In each case, these values are greater than those evaluated from Eq. 49 at the average albumin concentration in the polarization layer, $D = 1.2 \times 10^{-7}$ cm²/s for 350 g/L (Experiment D), $D = 1.8 \times 10^{-7}$ cm²/s for 250 g/L (Experiment B) and $D = 2.5 \times 10^{-7}$ cm²/s for 175 g/L (Experiment K). Larger values were also obtained in fitting the other concentration profiles and the magnitude of the difference between these diffusivities and those from Eq. 49 increased with increasing pH.

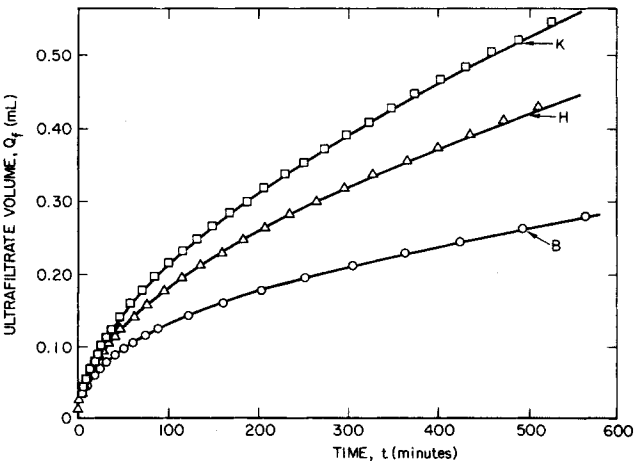

Figure 6. Measured ultrafiltrate volume as a function of elapsed time and bulk solution pH: Experiment K at pH 7.4 (□), Experiment H at pH 5.4 (△) and Experiment B at pH 4.5 (○). Applied pressure (ΔP = 70 kPa) and bulk solution albumin concentration (c_i = 101-110 g/L) were the same in the three experiments. Curves are regression fits for Eq. 50.

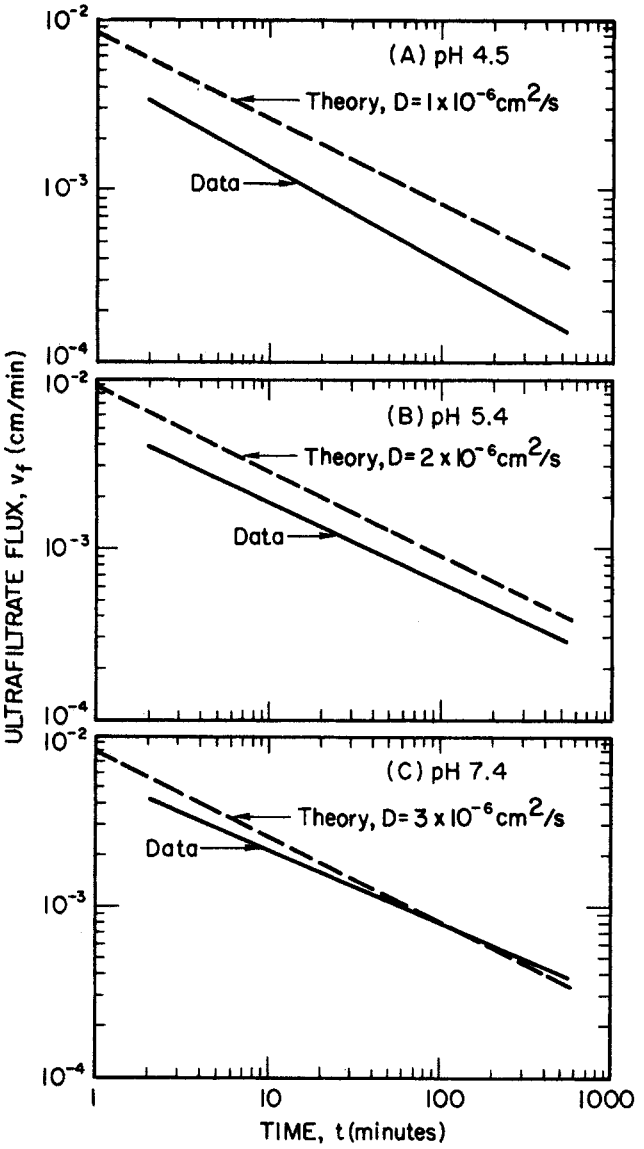

Figure 7. Measured ultrafiltrate flux decay (solid curves calculated from the derivative of Eq. 50 for three pH values: (A) Experiment B at pH 4.5, (B) Experiment H at pH 5.4 and (C) Experiment K at pH 7.4. Theoretical curves (dashed) calculated from $v_f = A_o t^{-1/2}$ where A_o is evaluated by Eq. 51 using the diffusivity which gave best fit to concentration profiles like those of Figure 5.

The polarization layer thickness δ is arbitrarily defined as the distance above the membrane at which the albumin concentration corresponds to $\theta_o = 0.02$. This thickness on Figure 5 is 0.260 for Experiment B, 0.375 cm for Experiment D and 0.400 for Experiment K. Profiles were measured at two different elapsed times in Experiments C and E to test the theoretical predictions that membrane surface concentration is nearly time invariant and that the polarization layer grows like $\sqrt{t}$. Within experimental error, the data for 542 and 1368 minutes of Experiment C and 33 and 88 minutes of Experiment E indicate that $c_s \simeq c^*$, independent of elapsed time of the experiment. The ratio of the polarization layer thickness at the longer elapsed time to that at the shorter time is in good agreement with the predicted $\sqrt{t}$ dependence for both experiments. However, comparisons of δ between experiments at different pH but otherwise nearly equivalent conditions and elapsed time show that δ increases as pH increases. This also indicates increasing apparent albumin diffusivities as the departure of pH from the isoelectric point increases.

Figure 6 shows typical results for the volume of ultrafiltrate produced as a function of elapsed time. The three sets of data plotted correspond to Experiments B, H, and K which differ only in the bulk solution pH. The curves drawn through the data represent nonlinear least squares regression fits to the equation

$$Q_f/A_m = \frac{A_o}{n+1} t^{n+1} \tag{50}$$

where Q_f is ultrafiltrate volume, A_m is the membrane area (1.524 cm²) and the parameters A_o and n are found from the regression analysis. Ultrafiltrate volume measurements began within three seconds after the start of an experiment. Because of substantial scatter in the data from the beginning of each run, regression analysis was carried out only with data obtained after two minutes elapsed time.

Figures 7a, 7b and 7c show plots of ultrafiltrate flux versus time for Experiments B, H and K, respectively, where the solid lines are calculated from the derivative of Eq. 50 after the constants A_o and n have been determined from regression analysis of the integral data. These constants for all experiments are listed in Table 1. The value of n is always close to the theoretical value of $-1/2$ but is somewhat less negative for experiments at higher pH. The value at low pressure for Experiment B agrees well with the higher pressure result at pH 4.5, Experiment D.

The ultrafiltrate flux data were also fit to Eq. 50 with n set equal to $-1/2$. The resulting A_o coefficients, shown in the second to last row of Table 1, are then related to albumin diffusivity by comparing the theoretical solution for v_f (Eqs. 7b and 9, and Figure 2) and Eq. 50:

$$A_o = V_o(\rho/\rho_f)\sqrt{D} \tag{51}$$

where the ratio of average polarization layer density to filtrate density (ρ/ρ_f) varied slightly for the experiments (1.04 to 1.09 g/mL). These diffusivities thus calculated from flux data are smaller and increase even more strongly with increasing solution pH than the values obtained by fitting the theoretical model, Eq. 21, to concentration profile data. Close agreement between the two sets of apparent diffusion coefficients is achieved only at pH 7.4. The dashed lines of Figures 7a, 7b and 7c show the ultrafiltrate flux decay computed from Eq. 51 where the value of V_o is from Figure 2 and the value of D is from the fit to the concentration profile of each respective experiment.

Thus, the general features of the ultrafiltration model are consistent with experimental data for both the ultrafiltrate flux and for the concentration profile. The apparently high values of the diffusivity reported in this study may in part be due to uncertainties as to the true value. The measurements leading to Eq. 49 by Keller et al. (1971) were taken at conditions (0.1 M acetate buffer, pH 4.7) such that albumin is near its isoelectric point (zero net molecular change) and the diffusivity was found to monotonically decrease with increasing concentration. A recent theoretical description predicts similar dependence when albumin is modeled as an inert hard sphere (Anderson and Reed, 1976). More recent albumin diffusivity measurements by quasielastic light scattering techniques suggest that diffusivity increases with concentration in solutions of pH (~7.4) and ionic strength (~0.1 M) such that electrostatic contributions significantly influence the concentration dependence (Phillies et al., 1976; Fair et al., 1978). These studies report values of the diffusivity approaching 10^{-6} cm²/s at the highest concentrations studied (~200 g/L).

We believe that the major portion of the discrepancy is associated with diffusion potential effects. This hypothesis is currently under investigation in our laboratory with encouraging results and will be reported in a subsequent paper.

ACKNOWLEDGMENT

Support was provided by NIH grants HL 14209 and HL 21429.

NOTATION

A_m = membrane area
A_o = flux fitting parameter defined by Eq. 50
B_g = gel layer permeability, cm²/kPa · min
c = albumin concentration, g/L solution
D = diffusivity, cm²/s
f = membrane pressure drop function defined by Eq. 39
L_p = membrane hydraulic permeability, cm/kPa · min
l_g = gel layer thickness
$\mathcal{L}$ = dimensionless gel layer thickness, $l_g/(Dt)^{1/2}$
N = albumin mass flux, g/cm² · min
n = flux fitting parameter defined by Eq. 50
ΔP = pressure differential, kPa
Pe_g = gel layer Peclet number, vl_g/D
Q_f = measured volume of ultrafiltrate
R = rejection coefficient for albumin defined by Eq. 5
t = time
V = dimensionless volumetric flux, $v\sqrt{t/D}$
v = volumetric flux, positive when flow is in negative y-direction, cm/min
y = coordinate normal to membrane

Greek Symbols

δ = polarization layer thickness
η = quantity defined by Eq. 11 or 31
θ = dimensionless concentration, $(c - c_i)/(c^* - c_i)$ or $(c - c_i)/(c_g - c_i)$
ξ = dimensionless polarization thickness defined by Eq. 10 or 30
π = osmotic pressure, kPa
ρ = mass density, g/mL
ϕ = albumin concentration as volume fraction
σ = membrane reflection coefficient for albumin

Subscripts

f = ultrafiltrate
g = gel layer
i = initial or bulk solution
m = membrne
o = denotes first term in series expansions of Eqs. 19-20 and 40-43
s = membrane surface

Superscripts

$*$ = condition at membrane surface when the product of the reflection coefficient and the osmotic pressure difference across the membrane equals the hydrostatic pressure difference

LITERATURE CITED

Alfani, F. and E. Drioli, "Concentration Polarization in an Unstirred Batch System," *Ing. Chim. Ital.*, **8**, 235 (1972).

Anderson, J. L. and J. A. Quinn, "Restricted Transport in Small Pores," *Biophys. J.*, **14**, 130 (1974).

Anderson, J. L. and C. C. Reed, "Diffusion of Spherical Macromolecules at Finite Concentration," *J. Chem. Phys.*, **64**, 3240 (1976).

Blatt, W. F., A. Dravid, A. S. Michaels and L. Nelson, "Solute Polarization and Cake Formation in Membrane Ultrafiltration: Causes, Consequences and Control Techniques," *Membrane Science and Technology*, J. E. Flinn, ed., Plenum Press, New York (1970).

Brown, C. E., M. P. Tulin and P. Van Dyke, "On the Gelling of High Molecular Weight Impermeable Solutes During Ultrafiltration," *CEP Symp. Ser.*, No. 114, **67**, 174 (1971).

Colton, C. K., S. Friedman, D. E. Wilson and R. S. Lees, "Ultrafiltration of Lipoproteins Through a Synthetic Membrane," *J. Clin. Invest.*, **5**, 2472 (1972).

Colton, C. K., L. W. Henderson, C. A. Ford and M. J. Lysaght, "Kinetics of Hemodiafiltration. I. In Vitro Transport Characteristics of a Hollow-Fiber Blood Ultrafilter," *J. Lab. Clin. Med.*, **85**, 355 (1975).

Dorson, W. J., V. B. Pizziconi and J. M. Allen, "Transfer of Chemical Species Through a Protein Gel," *Trans. Amer. Soc. Artif. Int. Organs*, **17**, 287 (1971).

Fair, B. D., D. Y. Chao and A. M. Jamieson, "Mutual Translational Diffusion Coefficients in Bovine Serum Albumin Solutions Measured by Quasielastic Laser Light Scattering," *J. Colloid Interface Sci.*, **66**, 323 (1978).

Henry, R. J., *Clinical Chemistry Principles and Techniques*, Harper and Row, New York, p. 190 (1964).

Keller, K. H., E. R. Canales and S. I. Yum, "Tracer and Mutual Diffusion Coefficients of Proteins," *J. Phys. Chem.*, **75**, 379 (1971).

Kozinski, A. A. and E. N. Lightfoot, "Protein Ultrafiltration: A General Example of Boundary Layer Filtration," *AIChE J.*, **18**, 1030 (1972).

Liu, M. K. and F. A. Williams, "Concentration Polarization in an Unstirred Batch Cell: Measurements and Comparison with Theory," *Int. J. Heat Mass Transfer*, **13**, 1441 (1970).

MacRitchie, F., "Effects of Temperature on Dissolution and Precipitation of Proteins and Polyamino Acids," *J. Colloid Interface Sci.*, **45**, 235 (1973).

Mahlab, D., N. B. Yosef and G. Belfort, "Concentration Polarization Profile for Dissolved Species in Unstirred Batch Hyperfiltration (Reverse Osmosis). II. Transient Case," *Desalination*, **24**, 297 (1978).

Mahlab, D., N. B. Yosef and G. Belfort, "Interferometric Measurement of Concentration Polarization Profile for Dissolved Species in Unstirred Batch Hyperfiltration (Reverse Osmosis)," 72nd Annual Meeting, AIChE, San Francisco (Nov. 25-29, 1979).

Michaels, A. S., "Ultrafiltration," *Progress in Separation and Purification*, S. Perry, ed., Interscience, New York, p. 297 (1968).

Nakao, S.-I., T. Nomura and S. Kimura, "Characteristics of Macromolecular Gel Layer Formed on Ultrafiltration Tubular Membrane," *AIChE J.*, **25**, 615 (1979).

Phillies, G. D. J., G. B. Benedek and N. A. Mazer, "Diffusion in Protein Solutions at High Concentrations: A Study by Quasielastic Light Scattering Spectroscopy," *J. Chem. Phys.*, **65**, 1883 (1976).

Porter, M. C. and L. Nelson, "Ultrafiltration in the Chemical, Food Processing, Pharmaceutical and Medical Industries," *Recent Developments in Separation Science*, **2**, N. N. Li, ed., CRC Press, Cleveland, OH (1972).

Shen, J. J. S. and R. F. Probstein, "On the Prediction of Limiting Flux in Laminar Ultrafiltration of Macromolecular Solutions," *Ind. Eng. Chem., Fundam.*, **16**, 459 (1977).

Spiegler, K. S. and O. Kedem, "Thermodynamics of Hyperfiltration (Reverse Osmosis): Criteria for Efficient Membranes," *Desalination*, **1**, 311 (1966).

Trettin, D. R. and M. R. Doshi, "Ultrafiltration in an Unstirred Batch Cell," *Ind. Eng. Chem. Fundam.*, **19**, 189 (1980).

Vilker, V. L., C. K. Colton, K. A. Smith, R. S. Lees and D. Green, "The Osmotic Pressure of BSA and Its Significance to Ultrafiltration," Paper 1d, 77th AIChE National Meeting, Pittsburgh (1974).

Vilker, V. L., "Ultrafiltration of Biological Macromolecules," Ph.D. Thesis, Massachusetts Institute of Technology, Cambridge (1975).

Vilker, V. L., C. K. Colton and K. A. Smith, "The Osmotic Pressure of Concentrated Protein Solutions: Analysis of Concentration and Solution pH Dependence for Bovine Serum Albumin in Saline Solutions," *J. Colloid Interface Sci.*, **79**, 548 (1981a).

Vilker, V. L., C. K. Colton and K. A. Smith, "Concentration Polarization in Protein Ultrafiltration. I. An Optical Shadowgraph Technique for Measuring Concentration Profiles Near a Solution-Membrane Interface," *AIChE J.* (July, 1981b).

Vilker, V. L., A. J. DiLeo, C. K. Colton and K. A. Smith, "Device for the Measurement of Small Liquid Flow Rates," *Rev. Sci. Instrum.*, **50**, 640 (1979).

Williams, F. A., "A Nonlinear Diffusion Problem Relevant to Desalination by Reverse Osmosis," *SIAM J. Appl. Math.*, **17**, 59 (1969).

Manuscript received June 3, 1980; revision received October 7, and accepted October 21, 1980.